NIH Public Access
Author Manuscript
Mol Cell Neurosci. Author manuscript; available in PMC 2012 December 23.

Published in final edited form as:
Mol Cell Neurosci. 2010 October ; 45(2): 173–179. doi:10.1016/j.mcn.2010.06.008.

Tyrosine phosphorylation regulates the membrane trafficking of the potassium chloride co-transporter KCC2

Henry H.C. Lee[a], **Rachel Jurd**[a], and **Stephen J. Moss**[a,b,*]

[a]Department of Neuroscience, Tufts University, Boston, MA 02111, USA

[b]Department of Neuroscience, Physiology and Pharmacology, University College, London WC1E 6BT, UK

Abstract

The activity of the neuronal-specific potassium chloride co-transporter KCC2 allows neurons to maintain low intracellular Cl^- concentrations. These low Cl^- concentrations are critical in mediating fast synaptic inhibition upon the activation of Cl^--permeable ligand-gated ion channels such as type A γ-aminobutyric acid receptors ($GABA_A$Rs). Deficits in KCC2 functional expression thus play central roles in the etiology of epilepsy and ischemia. It is emerging that KCC2 is phosphorylated on tyrosine residues, but the molecular substrates for this covalent modification within KCC2 and its functional significance remain poorly understood. Here we demonstrate that in HEK-293 cells the principal sites of tyrosine phosphorylation within KCC2 are residues 903 and 1087 (Y903/1087), which lie within the major C-terminal intracellular domain of KCC2. Phosphorylation of Y903/1087 decreases the cell surface stability of KCC2 principally by enhancing their lysozomal degradation. We further demonstrate that in cultured hippocampal neurons prolonged activation of muscarinic acetylcholine receptors (mAChRs) enhances KCC2 tyrosine phosphorylation and lysozomal degradation. Consistent with our *in vitro* studies, induction of status epilepticus (SE) in mice using pilocarpine, a mAChR agonist, induces large deficits in the cell surface stability of KCC2 together with enhanced tyrosine phosphorylation. Tyrosine phosphorylation of KCC2 is thus likely to play a key role in regulating the degradation of KCC2, a process that may be responsible for pathological losses of KCC2 function that are evident in SE and other forms of epilepsy.

Keywords

Potassium chloride co-transporter 2; Src-family tyrosine kinase; Cholinergic transmission; Epilepsy

Introduction

The neuronal-specific potassiumchloride co-transporter KCC2 plays an essential role in regulating intracellular Cl^- concentrations in the adult brain. The activity of KCC2 allows neurons to maintain low intracellular Cl^- concentrations, which is critical for efficient synaptic inhibition mediated by the activation of $GABA_A$Rs or glycine receptors (GlyRs) (Payne, 1997; Rivera et al., 1999). The essential role of KCC2 in mediating neuronal inhibition is illustrated in KCC2 null animals. KCC2 knock-out mice die shortly after birth.

*Corresponding author. Department of Neuroscience, Tufts University, Boston, MA 02111, USA. Stephen.Moss@tufts.edu (S.J. Moss).

Deficits in synaptic inhibition, especially the presence of depolarizing $GABA_AR$ responses, are evident (Hubner et al., 2001). Consistent with its role in Cl^- homeostasis, deficits in KCC2 functional expression are of significance in seizure disorders and excitotoxicity (Hekmat-Scafe et al., 2006; Pathak et al., 2007; Reid et al., 2001; Woo et al., 2002).

Given the critical role that KCC2 plays in neuronal function, there is considerable interest in how its functional expression is controlled. Much of the emphasis has been placed on the role of phosphorylation (Kahle et al., 2005; Kelsch et al., 2001; Lee et al., 2007; Wake et al., 2007; Watanabe et al., 2009). Phosphorylation of S940 in the intracellular C-terminal domain of KCC2, mediated by protein kinase C (PKC), stabilizes KCC2 on the neuronal cell surface and increases co-transporter activity (Lee et al., 2007). More recently, Rinehart et al. (2009) revealed that KCC2 is phosphorylated on threonine residues (T991 and T1048) by the serine/threonine kinase WNK1, which inhibits transporter activity without modifying receptor trafficking. Furthermore, oxidative stress has been reported to result in a rapid loss of tyrosine phosphorylation of KCC2 (Wake et al., 2007). Outward Cl^- transports mediated through KCC2 are also regulated by a cytosolic tyrosine kinase (Kelsch et al., 2001) and tyrosine receptor kinase B (TrkB) (Rivera et al., 2004). Tyrosine phosphorylation of KCC2 has also been implicated in the recruitment of this molecule into lipid rafts (Watanabe et al., 2009).

Here we demonstrate that the principal sites of tyrosine phosphorylation within KCC2 are Y903 and Y1087, which lie within the C-terminal intracellular domain of this critical transporter. Phosphorylation of Y903/1087 acts to decrease steady-state cell surface expression levels of KCC2 and leads to its subsequent lysozomal degradation, a process that is modulated via mAChRs. Finally, induction of SE leads to increased tyrosine phosphorylation and degradation of KCC2. Thus tyrosine phosphorylation may have profound effects on the functional expression of KCC2 under both physiological and pathological conditions.

Results

KCC2 is phosphorylated on two major tyrosine residues when expressed in HEK-293 cells

To identify sites of tyrosine phosphorylation within KCC2 we initially used recombinant expression in HEK-293 cells. 24–48 h after transfection, cells were treated with 100 μM sodium pervanadate to inhibit tyrosine dephosphorylation, lyzed, and subjected to immunoprecipitation with KCC2 antibodies. Precipitated material was immunoblotted with PY and KCC2 antibodies. It was found that immunoprecipitated KCC2 was phosphorylated at tyrosine residues (Fig. 1). No tyrosine phosphorylation was seen in the absence of sodium pervanadate pretreatment, presumably due to high levels of tyrosine phosphatase activity in HEK-293 cells (Moss et al., 1995).

To gain information on the molecular substrates of tyrosine phosphorylation within KCC2 we identified putative tyrosine kinase phosphorylation sites using the NetPhos 2.0 Server (http://www.cbs.dtu.dk/services/NetPhos/). This approach identified residues Y903 (SAYTYEKTL) and Y1087 (GDENYMEFL) within the C-terminal intracellular domain of KCC2 as possible substrates for phosphorylation. To test if these residues are actually phosphorylated the respective point mutants were engineered into the KCC2 full-length cDNA constructs and expressed in HEK-293 cells. Transfected cells were pre-treated with sodium pervanadate (100 μM, 30 min), lyzed, and subjected to immunoprecipitation followed by immunoblotting. The respective data were used to calculate the ratio of PY:KCC2 immunoreactivity for each construct. Mutations of Y903 or Y1087 to phenylalanine (Y903F and Y1087F) reduced tyrosine phosphorylation of KCC2 to 52 ± 12% and 70 ± 8.9% of wild-type (100%) respectively, suggesting that both sites are

phosphorylated (Fig. 1). A construct in which both residues were mutated (Y903/1087F) further reduced tyrosine phosphorylation of KCC2 to 26 ± 5.5% of wild-type (Fig. 1). These results indicate that Y903 and Y1087 are the major sites of tyrosine phosphorylation within KCC2.

Phosphorylation of Y903 and Y1087 modulates KCC2 stability in HEK-293 cells

Phosphorylation of KCC2 on serine residues can modulate the membrane trafficking of this transporter (Lee et al., 2007); thus we analyzed the possible role that tyrosine phosphorylation plays in regulating the cell surface stability of KCC2. To do so, HEK-293 cells transfected with KCC2 expression constructs for 24–48 h were treated with sodium pervanadate (100 μM, 30 min) and subjected to biotinylation before cell lysis. Cell surface and total protein fractions were immunoblotted with KCC2 antibody. Under these conditions sodium pervanadate treatment resulted in a significant reduction ($p<0.01$) in the cell surface and total populations of KCC2 to 65.5 ± 3.5% and 62.5 ± 3.5% of control respectively, without altering the abundance of tubulin (Fig. 2). The ratio of surface to total KCC2 also remained the same after sodium pervanadate treatment (Fig. 2), suggesting that the loss of cell surface KCC2 is associated with the loss of total KCC2. In contrast, the cell surface or total expression levels of a mutant version of KCC2 in which both Y903 and Y1087 were mutated to phenylalanine residues (Y903/1087F) were not significantly different from control after treatment with sodium pervanadate. We also compared the steady-state expression levels of wild-type and Y903/1087F and, consistent with a role for tyrosine phosphorylation in decreasing the stability of KCC2, mutation of Y903/1087 increased both the cell surface and total expression levels of KCC2 (Fig. 2). Interestingly, single mutation of Y903 or Y1087 to phenylalanine did not significantly modify sodium pervanadate-induced degradation of KCC2 (Fig. 2), suggesting that both participate in phospho-dependent degradation of KCC2.

Tyrosine phosphorylation by Src-family tyrosine kinases regulates the stability of KCC2 in neurons

To examine the significance of our recombinant experiments we examined whether KCC2 is phosphorylated on tyrosine residues in cultured neurons. To do so hippocampal primary cultures were treated with sodium pervanadate (100 μM, 30 min) and subjected to immunoprecipitation with KCC2 antibodies. Precipitated material was immunoblotted with PY and KCC2 antibodies. Under basal conditions, negligible tyrosine phosphorylation of KCC2 was evident; however, exposure to sodium pervanadate induced a robust tyrosine phosphorylation of KCC2 (Fig. 3A). To gain insights into the kinase(s) that mediate KCC2 tyrosine phosphorylation, sodium pervanadate-treated neurons were exposed to PP2, a potent inhibitor of Src-family tyrosine kinases. PP2, but not the inactive control compound PP3, ablated sodium pervanadate-induced tyrosine phosphorylation of KCC2 and degradation of KCC2 (Fig. 3B). In addition, the amount of cell surface KCC2 was higher in PP2-treated neurons than those in control conditions, further supporting the hypothesis that tyrosine phosphorylation of KCC2 regulates its cell surface expression in neurons. Taken together, Src-family tyrosine kinases likely modulate the tyrosine phosphorylation and degradation of KCC2 in neurons.

To examine if tyrosine phosphorylation modifies the expression levels of KCC2, cultured hippocampal neurons were treated with sodium pervanadate and the effects on the total and cell surface expression levels of KCC2 were measured (Lee et al., 2007). Prolonged treatment of neurons with sodium pervanadate (100 μM, 30 min) reduced the total and cell surface populations of KCC2 to 48 ± 3.9% and 58 ± 14% of control respectively without altering the stability of tubulin (Fig. 4A).

Tyrosine phosphorylation primarily acts to increase the lysozomal degradation of KCC2

Previous studies have revealed that KCC2 molecules undergo high levels of constitutive endocytosis (Lee et al., 2007); thus to further understand the mechanism by which tyrosine phosphorylation regulates the degradation of KCC2, we focused on possible changes in the trafficking of this molecule in the endocytic pathway. To do so we first examined the effects of blocking clathrin-dependent endocytosis or lysozomal degradation on the cell surface and total expression levels of KCC2. Treatment of neurons with dynasore (80 μM) a membrane-permeable inhibitor of dynamin (Macia et al., 2006) increased the cell surface and total expression levels of KCC2 to 275 ± 16% and 155 ± 4% of control respectively within 45 min. Likewise treatment of neurons with leupeptin (200 μg/ml) over the same time course increased cell surface and total levels of KCC2 to 185 ± 10% and 175 ± 8% of control respectively. Under the same conditions there was minimal effect on the stability of tubulin. Blocking either clathrin-dependent endocytosis or lysozomal degradation thus rapidly increases the cell surface accumulation and total expression levels of KCC2. This indicates high basal rates of clathrin-dependent endocytosis and lysozomal degradation and provides a mechanism to explain the short cell surface half-life of KCC2 as reported by Rivera et al. (2004).

We next went on to test the effects of leupeptin and dynasore on pervanadate-induced degradation of KCC2. Pretreatment with leupeptin (200 μg/ml, 15 min) ameliorated pervanadate-induced degradation of both cell surface and total populations of KCC2. Dynasore treatment largely blocked the pervanadate-induced degradation of the cell surface population KCC2 but did not modify degradation of the total cellular pool of KCC2. These results suggest that pervanadate acts primarily to regulate the lysozomal degradation of KCC2. The ability of dynasore to block the effects of pervanadate on cell surface populations presumably reflects reduced entry of KCC2 into the endocytic pathway which precedes trafficking to the lysozome for degradation.

mAChRs modulate the tyrosine phosphorylation and degradation of KCC2

To examine the upstream signaling pathways that regulate KCC2 tyrosine phosphorylation in neurons we focused on mAChRs, as these G-protein coupled receptors are potent activators of tyrosine phosphorylation signaling pathways (Ma et al., 2003). Their prolonged activation also leads to the induction of SE and profound decreases in the functional expression of KCC2 in rodents (Kapur and Coulter, 1995; Pathak et al., 2007; Rivera et al., 1999). For these experiments, hippocampal cultures were treated with carbachol, a muscarinic agonist, in the absence and presence of sodium pervanadate. Carbachol treatment (100 μM, 30 min) together with sodium pervanadate (100 μM, 30 min) induced a significant increase ($p<0.01$) in the level of tyrosine phosphorylation of KCC2 compared to cultures treated with sodium pervanadate alone (165 ± 5.6% of control, Fig. 5). The total amount of KCC2 was significantly reduced ($p<0.01$) in cultures treated with sodium pervanadate alone or with the addition of carbachol (Fig. 5). These data corroborate our previous recombinant data showing that tyrosine phosphorylation of KCC2 decreases its stability. We also examined the effects of carbachol alone on the stability of KCC2. As illustrated in Fig. 6, carbachol treatment (60 min) significantly reduced the cell surface levels and total expression levels of KCC2 to 70 ± 3% and 72.5 ± 2.5% respectively compared to control without modifying the levels of tubulin. Together these results indicate that prolonged activation of mAChRs promotes the tyrosine phosphorylation and degradation of KCC2.

SE induces tyrosine phosphorylation and degradation of KCC2

It is widely accepted that muscarinic agonists induce SE, which leads to reduced KCC2 expression levels (Kapur and Coulter, 1995; Pathak et al., 2007); thus we tested whether induction of SE using pilocarpine, a mAChR agonist, modifies the tyrosine phosphorylation

of KCC2. To do so mice were injected with 330 mg/kg pilocarpine and mice exhibiting stage 5 seizures were sacrificed after 60 min (Terunuma et al., 2008). 350 μm hippocampal slices were then incubated in ACSF (bubbled with 95% O_2/5% CO_2) for 1 h at 32 °C before being labeled with NHS-biotin and, after purification on immobilized avidin, cell surface and total fractions were immunoblotted with KCC2 antibodies. To control for membrane integrity after generation of brain slices, cell surface and total fractions were immunoblotted with tubulin antibodies. The tubulin signal in the biotinylated fraction of proteins was at least 100-fold less intense than that of the total protein fraction for inclusion of data. Acute brain slices were also used in immunoprecipitation with KCC2 and tyrosine phosphorylation investigated by immunodetection using PY antibodies. In slices derived from animals undergoing SE there was a significant increase in tyrosine phosphorylation of KCC2 (Fig. 7). Consonant with this data, both cell surface and total amount of KCC2 were dramatically reduced in slices generated from SE animals to 73 ± 2% and 58 ± 4% of control respectively, without altering the amount of tubulin (Fig. 7).

Discussion

The ability of neurons to maintain low intracellular Cl^- levels is a prerequisite for efficient inhibitory neurotransmission upon the activation of $GABA_A$Rs and GlyRs. This property is dependent largely upon the activity of KCC2, which is the principal Cl^- extruder in mature neurons. KCC2 activity is subject to phosphorylation by a number of serine/threonine protein kinases at sites within the C-terminal cytoplasmic domain. These modifications regulate transporter membrane trafficking and activity (Kahle et al., 2005; Lee et al., 2007; Strange et al., 2000). KCC2 is also subject to tyrosine phosphorylation (Wake et al., 2007; Watanabe et al., 2009), but the sites for this covalent modification within KCC2 and the molecular consequences of their phosphorylation remain to be determined.

To address this issue, we used recombinant expression of KCC2 in HEK-293 cells. This system has been used in our previous studies of protein trafficking and degradation of KCC2 (Lee et al., 2007). Inhibition of tyrosine phosphatases by pretreatment of transfected cells with sodium pervanadate resulted in robust tyrosine phosphorylation of KCC2. We identified two residues within the C-terminal cytoplasmic intracellular domain of KCC2 (Y903 and Y1087) that, when mutated to phenylalanine, reduced tyrosine phosphorylation of KCC2 to 20% of control levels. Y903 and Y1087 are thus likely to represent the principal sites of tyrosine phosphorylation in KCC2. Other tyrosine phosphorylation sites may be present on KCC2; however, given their relatively low levels of phosphorylation compared to Y903 and Y1087, they are likely to play minor roles in the protein degradation of KCC2. To our knowledge, our current findings are the first demonstration that these residues are actually phosphorylated.

We next explored the functional consequences of tyrosine phosphorylation of KCC2. Previous studies suggested that inhibition of tyrosine kinase leads to inhibition of KCC2 (Kelsch et al., 2001). However, a direct relationship between phosphorylation level of KCC2 and its activities was not studied. In our experiments we first demonstrated a direct correlation between tyrosine phosphorylation and degradation of KCC2. Pretreatment of KCC2-transfected HEK-293 cells or cultured neurons with sodium pervanadate resulted in a decrease in both the cell surface and total expression levels of KCC2. In addition, using specific inhibitors of Src-family tyrosine kinases, KCC2 degradation induced by tyrosine phosphorylation was blocked. Thus tyrosine phosphorylation of KCC2 enhances the degradation of KCC2. Interestingly, Y1087 has previously been implicated in the functional modulation of KCC2 but not the alteration in its cell surface expression (Strange et al., 2000). This discrepancy may be due to the difference in the culture system used (oocytes in the previous study vs HEK-293 cells in our present study). In another study the researchers

described how oxidative stress decreases KCC2 co-transport activity through tyrosine dephosphorylation of KCC2 (Wake et al., 2007). These seemingly contradictory results compared to our present study can be explained by the fact that in the previous study oxidative stress increased both tyrosine phosphorylation and dephosphorylation (i.e. turnover) of KCC2, which in turn reduced cell surface expression of KCC2 (Wake et al., 2007). Oxidative stress may well exert an effect on other kinase/phosphatase systems to regulate KCC2 cell surface stability (Lee et al., 2007).

To assess whether phosphorylation of these residues Y903/1087 in KCC2 is directly related to degradation of KCC2 we used a mutant construct in which these residues were mutated to phenylalanines. Mutation of these residues significantly reduced the level of degradation of KCC2 compared to the degradation observed for wild-type KCC2, and the respective mutant exhibited higher steady-state accumulation levels in HEK-293 cells. This mutant is resistant to degradation induced by sodium pervanadate treatment. Interestingly, single mutation of these residues (Y903F or Y1087F) is sensitive to sodium pervanadate treatment, suggesting that both residues are involved in the phosphorylation-dependent degradation of KCC2.

The significance of tyrosine phosphorylation for endogenous KCC2 molecules in hippocampal neurons was also examined. Pretreatment of cultured hippocampal neurons with sodium pervanadate induced significant levels of KCC2 tyrosine phosphorylation. This enhancement of tyrosine phosphorylation was blocked by the pharmacological inhibition of Src-family tyrosine kinases, suggesting that tyrosine phosphorylation of KCC2 is dependent on one or more kinases from this particular family. We used PP3, an inactive structural analog of PP2, as a control. This clearly indicated that tyrosine phosphorylation of KCC2 is mediated specifically by Src-family tyrosine kinases. In keeping with our recombinant studies, enhanced tyrosine phosphorylation correlated with a significant decrease in both cell surface and total expression levels of KCC2, an effect that could be abrogated by leupeptin. Given the rapid turnover of surface KCC2 (Lee et al., 2007; Rivera et al., 2004), endocytosed KCC2 can either be degraded or re-inserted into the cell surface. These results obtained with leupeptin suggest that tyrosine phosphorylation targets KCC2 for lysozomal degradation. In the presence of leupeptin, lysozomal degradation was blocked, thereby increasing the intracellular pool of KCC2 and promoting re-insertion of KCC2 back onto the cell surface. This in turn blocked the downregulation of surface KCC2. This finding is further supported by the fact that dynasore, a dynamin inhibitor that inhibits clathrin-mediated endocytosis, did not prevent degradation of KCC2 after treatment with sodium pervanadate, suggesting that tyrosine phosphorylation targets internalized KCC2 for lysozomal degradation.

We further analyzed the signaling molecules that modulate KCC2 tyrosine phosphorylation, focusing on the possible role of mAChRs, as these receptors are potent modulators of tyrosine phosphorylation signaling pathways (Ma et al., 2003). This revealed that activation of mAChRs induced tyrosine phosphorylation of KCC2 and subsequent degradation. The prolonged activation of mAChRs with low efficacious agonists such as pilocarpine induces SE and decreases KCC2 activity in rodents (Kapur and Coulter, 1995; Pathak et al., 2007); thus we assessed the effects of SE induced by pilocarpine on the tyrosine phosphorylation and stability of KCC2. Consistent with our *in vitro* experiments, induction of SE produced a dramatic increase in KCC2 tyrosine phosphorylation and a reduction in the cell surface stability of this molecule. However, it was also noted that some animals did not develop SE nor did they exhibit tyrosine phosphorylation and degradation of KCC2 after injection of pilocarpine. This suggests that other cellular mechanisms may be present (Lee et al., 2007) to counteract tyrosine phosphorylation and subsequent degradation of KCC2 upon muscarinic activation. Nevertheless, tyrosine phosphorylation of KCC2 and its degradation suggests that a cause–effect relationship underlies the development of SE in animals.

Our studies have identified Y903/1087 as specific sites for tyrosine phosphorylation within KCC2 and suggested that their phosphorylation regulates the stability of KCC2 by promoting their lysozomal degradation, a process that is regulated by mAChRs. The induction of SE leads to increased tyrosine phosphorylation and degradation of KCC2. Enhanced tyrosine phosphorylation of KCC2 may thus be a potential mechanism underlying pathological rises in intracellular Cl^- levels during SE (Pathak et al., 2007). Inhibiting KCC2 tyrosine phosphorylation may represent a novel therapeutic approach to restore aberrant neuronal inhibition and limit epileptiform activity.

Experimental methods

Antibodies

A mouse monoclonal KCC2 antibody raised against the C-terminal intracellular domain (aa 932 to aa 1043) (1:1000 dilution, Antibodies Incorporated) was used for western blotting. A rabbit polyclonal KCC2 antibody (Millipore) was used in immunoprecipitation. Tyrosine phosphorylation was detected using the monoclonal phospho-tyrosine (PY) antibody 4G10 (1:1000 dilution, Millipore) after immunoprecipitation of KCC2. Tubulin antibodies (1:5000 dilution, Sigma) were used as protein loading control for all experiments.

Drug treatments

Sodium pervanadate was prepared freshly on the day of treatment. Briefly, a 30 mM solution of sodium orthovanadate (Sigma)was activated by the addition of hydrogen peroxide (0.2% final concentration) and incubated for at least 15 min before use. Carbachol (Tocris) was diluted in water to make a 100 mM stock solution. Leupeptin (Tocris) was diluted in water to make a 10 mg/ml stock solution. Dynasore (Tocris) was diluted in dimethyl sulfoxide (Sigma) to make an 80 mM stock solution. Scopolamine methyl nitrate (Sigma) was diluted freshly in water to make a 0.5 mg/ml solution. Pilocarpine hydrochloride (Sigma) was diluted freshly in water to make a 165 mg/ml solution. All stock solutions were kept at −80 °C for storage if necessary.

Immunoblotting and immunoprecipitation

Protein from cultured cells was extracted using lysis buffer containing (in mM): 10 $NaPO_4$, 5 EGTA, 5 EDTA, 10 Na pyrophosphate, 1 Na orthovanadate, 100 NaCl, 25 NaF, 2% Triton X-100 and 0.5% deoxycholate. Protease inhibitors leupeptin, pepstatin (Sigma), and aprotinin (Sigma) (10 μg/ml) were added freshly before cell lysis. Cell lysates were centrifuged using a benchtop microcentrifuge at 13,200 rpm at 4 °C for 10 min to get rid of insoluble materials. Extracted proteins were then separated by SDS-PAGE and transferred to a nitrocellulose membrane for detection of proteins by immunoblotting as described previously (Lee et al., 2007). Immunoprecipitation of proteins was performed as described previously (Kittler et al., 2000). Cell lysates or homogenates from acute hippocampal slices of SE mice (200 μg) were incubated with 2 μg rabbit polyclonal KCC2 antibodies (Millipore) and 40 μl of 1:1 slurry of protein A sepharose CL-4B beads (Amersham) in 1× PBS at 4 °C on a rotating wheel for 2 h. The beads were spun down at 4000 rpm for 2 min and washed twice with lysis buffer containing 0.5 M NaCl and once with normal lysis buffer. Supernatant was removed after centrifugation and 20 μl of SDS sample buffer was added to the beads. The sample was then analyzed using SDS-PAGE.

Biotinylation

Cell surface protein labeling using biotinylation was performed as described previously (Lee et al., 2007). Briefly, HEK-293 cells transfected with KCC2 constructs or cultured neurons were washed 2 times with PBS containing 0.5 mM $MgCl_2$ and 1 mM $CaCl_2$ (PBS-CM) and

then incubated with 2 ml of PBS-CM containing 1 mg/ml Sulfo-NHS-SS-Biotin (Pierce) for 30 min at 4 °C. After labeling, the biotin reaction was quenched by washing 3 times with ice-cold PBS-CM containing 50 mM glycine and 0.1% bovine serum albumin. Cells were then lyzed with 1 ml lysis buffer and the supernatant was collected. Protein concentration was determined using Micro BCA protein assay kit (Thermo Scientific). After correction for protein contents, 40 μl of 1:1 slurry of UltraLink NeutrAvidin (Pierce) was added to the supernatants to pull down the biotin-labeled surface proteins for 2 h at 4 °C. The NeutrAvidin beads were washed and bound materials were analyzed by SDS-PAGE. Acute hippocampal slices from SE mice were similarly labeled with 1 mg/ml Sulfo-NHS-SS-Biotin in artificial cerebrospinal fluid (ACSF, see below for components) for 30 min at 4 °C after a 1 h recovery period at 32 °C. Excess biotin was washed 3 times using ice-cold ACSF. Slices were then lyzed and homogenized. After centrifugation and correction for protein contents, biotin-labeled surface proteins were pulled down using NeutrAvidin and analyzed by SDS-PAGE.

Molecular cloning

Recombinant full-length KCC2 cDNA was subcloned into pRK5 mammalian expression vector as described previously (Lee et al., 2007). Site-directed mutagenesis of tyrosine residues to phenylalanine was performed using the Stratagene QuikChange method. For mutation of Y903 the following primers were used: (sense) GACATCTCAGCATACACCTTCGAGAAGACATTGGTAA; (antisense) TTACCAATGTCTTCTCGAAGGTGTATGCTGAGATGTC. For mutation of Y1087: (sense) AACTTCATGGAATTCCTGGAG; (antisense) TTCATCTCCATTGCGGTTG. Cultured HEK-293 cells were transiently transfected using electroporation as described previously (Lee et al., 2007) and cells were utilized 24–48 h after transfection.

Cultured neurons

Hippocampal neurons were dissected from rat embryos at embryonic day 18 as described previously (Lee et al., 2007). Cultures were maintained in a neurobasal medium supplemented with B-27 neural supplement and 2 mM L-glutamine for 3 weeks before the experiments.

Induction of SE

Adult FVB/N mice (8–12 weeks old, The Jackson Laboratory) were injected with scopolamine methyl nitrate (0.5 mg/ml, Sigma) subcutaneously at a dose of 1 mg/kg to minimize the peripheral cholinergic effects of pilocarpine. Thirty minutes later, pilocarpine hydrochloride (165 mg/ml, Sigma) was injected subcutaneously at a dose of 330 mg/kg to induce seizures. Continuous seizures were observed for 1 h before the animals were sacrificed and brains were dissected quickly for biochemical analysis. Animals injected with saline or those injected with pilocarpine but in which no seizures developed were used as controls.

Preparation of acute brain slices

Adult FVB/N mice (Jackson Laboratories) that developed SE for 1 h after pilocarpine injection were deeply anesthetized with isoflurane and decapitated. The hippocampus was then quickly removed and rinsed with ice-cold ACSF containing (in mM): 124 NaCl, 3 KCl, 25 $NaHCO_3$, 2 $CaCl_2$, 1.1 NaH_2PO_4, 2 $MgSO_4$ and 10 glucose, equilibrated with 95% O_2/5% CO_2 to yield a pH of 7.4. The hippocampus was then cut into 350 μm slices using a vibratome (VT1000S, Leica) for slice biotinylation. Acute hippocampal slices were incubated in ACSF at 32 °C for 1 h to recover before the experiments.

Statistical analysis

All data derived from experiments described in this report were analyzed as described previously (Lee et al., 2007). The MultiGauge program (Fujifilm) was used for the quantification of all immunoblots. Standard error of the mean (SEM) was calculated using Microsoft Office Excel 2003 from quantified data. Student's t-test was then performed using GraphPad Prism 4 for analysis of statistical significance.

Acknowledgments

This work was supported in part by NIH/NINDS grants NS-036296, NS-047478, NS-048045 and NS-054900. HHCL is supported by a fellowship from the American Heart Association. RJ is supported by the Maltz Family Foundation as a National Alliance for Research on Schizophrenia and Depression Young Investigator.

References

Hekmat-Scafe DS, Lundy MY, Ranga R, Tanouye MA. Mutations in the K+/Cl− cotransporter gene kazachoc (kcc) increase seizure susceptibility in *Drosophila*. J. Neurosci. 2006; 26:8943–8954. [PubMed: 16943550]

Hubner CA, Stein V, Hermans-Borgmeyer I, Meyer T, Ballanyi K, Jentsch TJ. Disruption of KCC2 reveals an essential role of K-Cl cotransport already in early synaptic inhibition. Neuron. 2001; 30:515–524. [PubMed: 11395011]

Kahle KT, Rinehart J, de Los Heros P, Louvi A, Meade P, Vazquez N, Hebert SC, Gamba G, Gimenez I, Lifton RP. WNK3 modulates transport of Cl− in and out of cells: implications for control of cell volume and neuronal excitability. Proc. Natl. Acad. Sci. U. S. A. 2005; 102:16783–16788. [PubMed: 16275911]

Kapur J, Coulter DA. Experimental status epilepticus alters gamma-aminobutyric acid type A receptor function in CA1 pyramidal neurons. Ann. Neurol. 1995; 38:893–900. [PubMed: 8526461]

Kelsch W, Hormuzdi S, Straube E, Lewen A, Monyer H, Misgeld U. Insulin-like growth factor 1 and a cytosolic tyrosine kinase activate chloride outward transport during maturation of hippocampal neurons. J. Neurosci. 2001; 21:8339–8347. [PubMed: 11606621]

Kittler JT, Delmas P, Jovanovic JN, Brown DA, Smart TG, Moss SJ. Constitutive endocytosis of GABAA receptors by an association with the adaptin AP2 complex modulates inhibitory synaptic currents in hippocampal neurons. J. Neurosci. 2000; 20:7972–7977. [PubMed: 11050117]

Lee HH, Walker JA, Williams JR, Goodier RJ, Payne JA, Moss SJ. Direct protein kinase C-dependent phosphorylation regulates the cell surface stability and activity of the potassium chloride cotransporter KCC2. J. Biol. Chem. 2007; 282:29777–29784. [PubMed: 17693402]

Ma XH, Zhong P, Gu Z, Feng J, Yan Z. Muscarinic potentiation of GABA(A) receptor currents is gated by insulin signaling in the prefrontal cortex. J. Neurosci. 2003; 23:1159–1168. [PubMed: 12598604]

Macia E, Ehrlich M, Massol R, Boucrot E, Brunner C, Kirchhausen T. Dynasore, a cell-permeable inhibitor of dynamin. Dev. Cell. 2006; 10:839–850. [PubMed: 16740485]

Moss SJ, Gorrie GH, Amato A, Smart TG. Modulation of GABAA receptors by tyrosine phosphorylation. Nature. 1995; 377:344–348. [PubMed: 7566089]

Pathak HR, Weissinger F, Terunuma M, Carlson GC, Hsu FC, Moss SJ, Coulter DA. Disrupted dentate granule cell chloride regulation enhances synaptic excitability during development of temporal lobe epilepsy. J. Neurosci. 2007; 27:14012–14022. [PubMed: 18094240]

Payne JA. Functional characterization of the neuronal-specific K-Cl cotransporter: implications for [K+]o regulation. Am. J. Physiol. 1997; 273:C1516–C1525. [PubMed: 9374636]

Reid KH, Li GY, Payne RS, Schurr A, Cooper NG. The mRNA level of the potassium–chloride cotransporter KCC2 covarieswith seizure susceptibility in inferior colliculus of thepost-ischemic audiogenic seizure-prone rat. Neurosci. Lett. 2001; 308:29–32. [PubMed: 11445278]

Rinehart J, et al. Sites of regulated phosphorylation that control K–Cl cotransporter activity. Cell. 2009; 138:525–536. [PubMed: 19665974]

Rivera C, Voipio J, Payne JA, Ruusuvuori E, Lahtinen H, Lamsa K, Pirvola U, Saarma M, Kaila K. The K+/Cl− co-transporter KCC2 renders GABA hyperpolarizing during neuronal maturation. Nature. 1999; 397:251–255. [PubMed: 9930699]

Rivera C, Voipio J, Thomas-Crusells J, Li H, Emri Z, Sipila S, Payne JA, Minichiello L, Saarma M, Kaila K. Mechanism of activity-dependent downregulation of the neuron-specific K-Cl cotransporter KCC2. J. Neurosci. 2004; 24:4683–4691. [PubMed: 15140939]

Strange K, Singer TD, Morrison R, Delpire E. Dependence of KCC2 K-Cl cotransporter activity on a conserved carboxy terminus tyrosine residue. Am. J. Physiol. 2000; 279:C860–C867.

Terunuma M, Xu J, Vithlani M, Sieghart W, Kittler J, Pangalos M, Haydon PG, Coulter DA, Moss SJ. Deficits in phosphorylation of GABA(A) receptors by intimately associated protein kinase C activity underlie compromised synaptic inhibition during status epilepticus. J. Neurosci. 2008; 28:376–384. [PubMed: 18184780]

Wake H, Watanabe M, Moorhouse AJ, Kanematsu T, Horibe S, Matsukawa N, Asai K, Ojika K, Hirata M, Nabekura J. Early changes in KCC2 phosphorylation in response to neuronal stress result in functional downregulation. J. Neurosci. 2007; 27:1642–1650. [PubMed: 17301172]

Watanabe M, Wake H, Moorhouse AJ, Nabekura J. Clustering of neuronal K+-Cl− cotransporters in lipid rafts by tyrosine phosphorylation. J. Biol. Chem. 2009; 284:27980–27988. [PubMed: 19679663]

Woo NS, Lu J, England R, McClellan R, Dufour S, Mount DB, Deutch AY, Lovinger DM, Delpire E. Hyperexcitability and epilepsy associated with disruption of the mouse neuronal-specific K-Cl cotransporter gene. Hippocampus. 2002; 12:258–268. [PubMed: 12000122]

Glossary

ACSF	artificial cerebrospinal fluid
CCh	carbachol
$GABA_AR$	γ-aminobutyric acid receptor type A
GlyR	glycine receptor
HEK	human embryonic kidney
KCC2	K^+ Cl^- co-transporter 2
kDa	kiloDalton
mAChR	muscarinic acetylcholine receptor
PBS	phosphate-buffered saline
PKC	protein kinase C
PY	phospho-tyrosine
SDS-PAGE	sodium dodecyl sulphate-polyacrylamide gel electrophoresis
SE	status epilepticus
SEM	standard error of the mean
TyrY	tyrosine
VO_4	sodium pervanadate
WNK1	with-no-lysine kinase 1
WT	wild-type

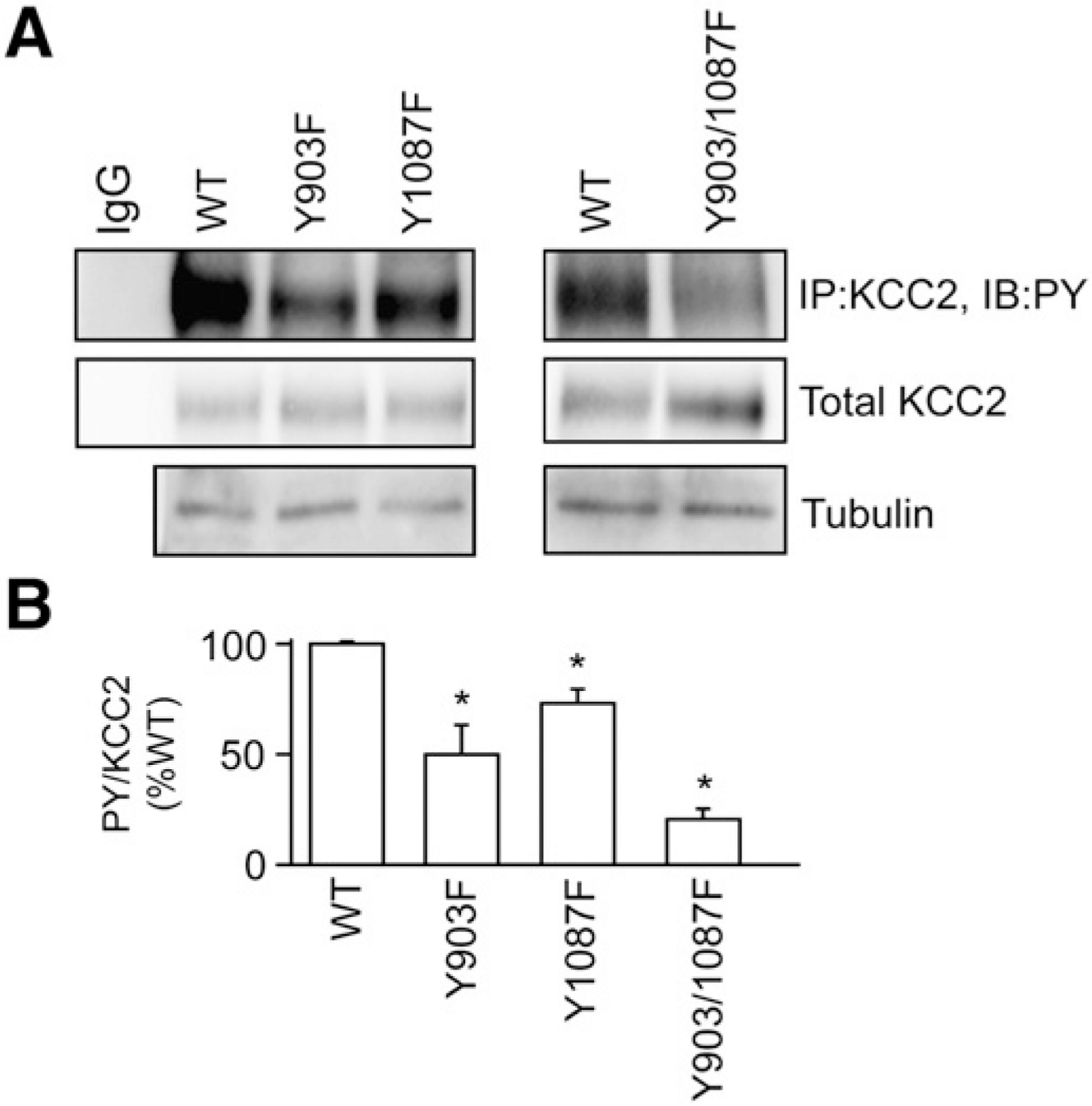

Fig. 1.

Tyrosine phosphorylation of KCC2 occurs on two residues. A. HEK-293 cells were transfected with full-length KCC2 wild-type (WT), Y903F, Y1087F or Y903/1087F cDNA constructs. Cells were treated with sodium pervanadate (VO_4, 100 μM, 30 min) followed by lysis and immunoprecipitation of KCC2. Immunoblotting with PY antibodies revealed the level of tyrosine phosphorylation of the different mutant constructs. Blots were also incubated with KCC2 antibodies to detect the total KCC2 level. In addition total extracts were immunoblotted with tubulin antibodies. Non-specific IgG was used as control for immunoprecipitation. B. The ratio of PY/KCC2 immunoreactivity was then determined and

normalized to control. [*Significantly different from WT ($p<0.01$; value = mean ± SEM, Student's t-test, n=3)].

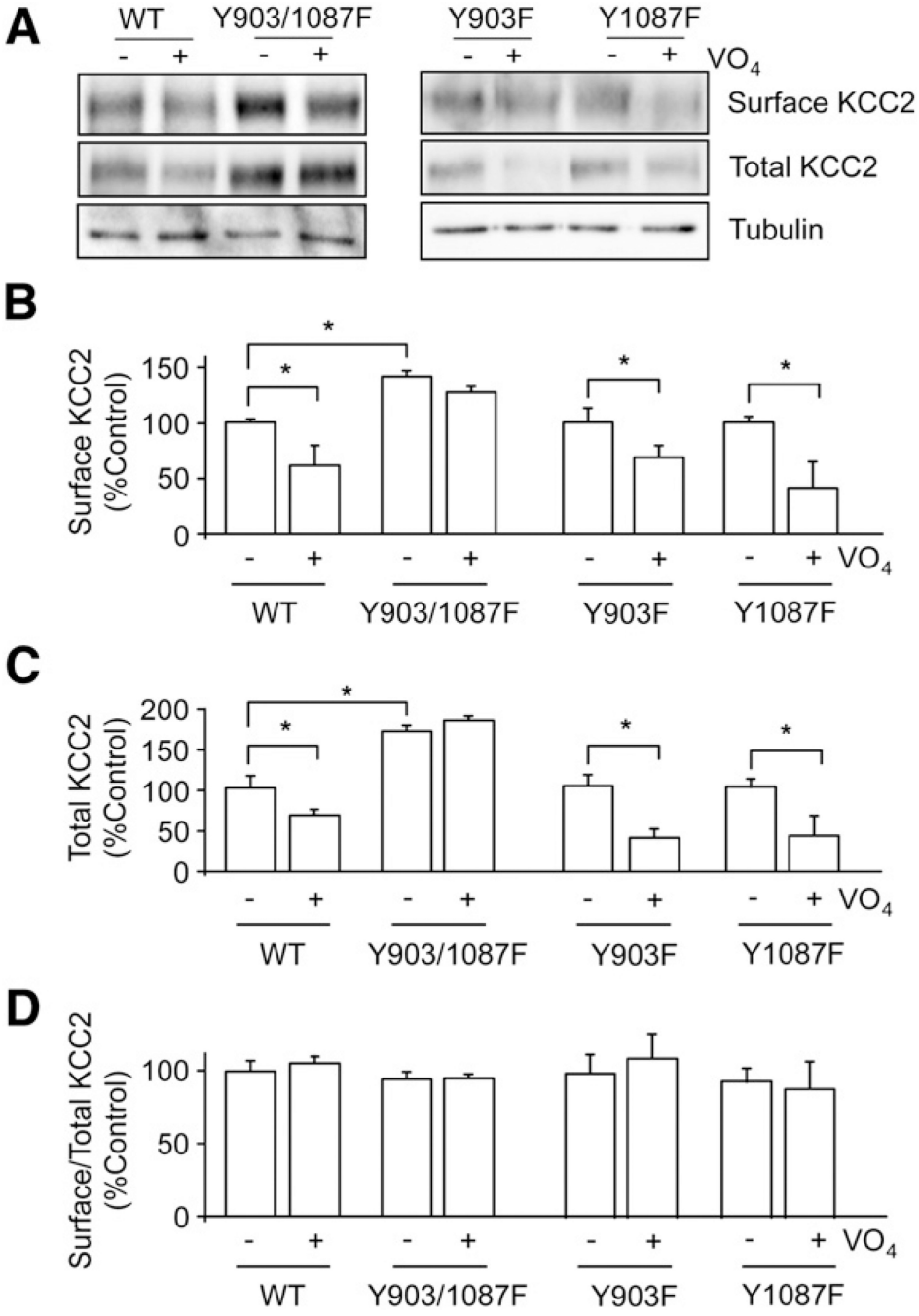

Fig. 2.

Tyrosine phosphorylation of KCC2 at Y903 and Y1087 is important for cell surface stability and total protein stability of KCC2. A. KCC2 wild-type (WT), double mutant Y903/1087F, and single mutant Y903F or Y1087F cDNAs were expressed in HEK-293 cells. Transfected cells were pre-treated with (+) or without (−) sodium pervanadate (VO_4, 100 μM, 30 min). The cell surface levels of KCC2 proteins at steady-state were measured using biotinylation followed by immunoblotting. Total extracts were immunoblotted with tubulin antibodies to control for loading. The cell surface levels of KCC2 were then measured with (+) or without (−) VO_4 treatment. B. Total KCC2 proteins levels (C) and the ratio of cell surface/total KCC2 were determined (D) and normalized to control (−Vn). Tubulin antibodies were used

in immunoblotting to show equal loading of proteins. [*Significantly different from control condition ($p<0.01$; value = mean ± SEM, Student's t-test, n=3)].

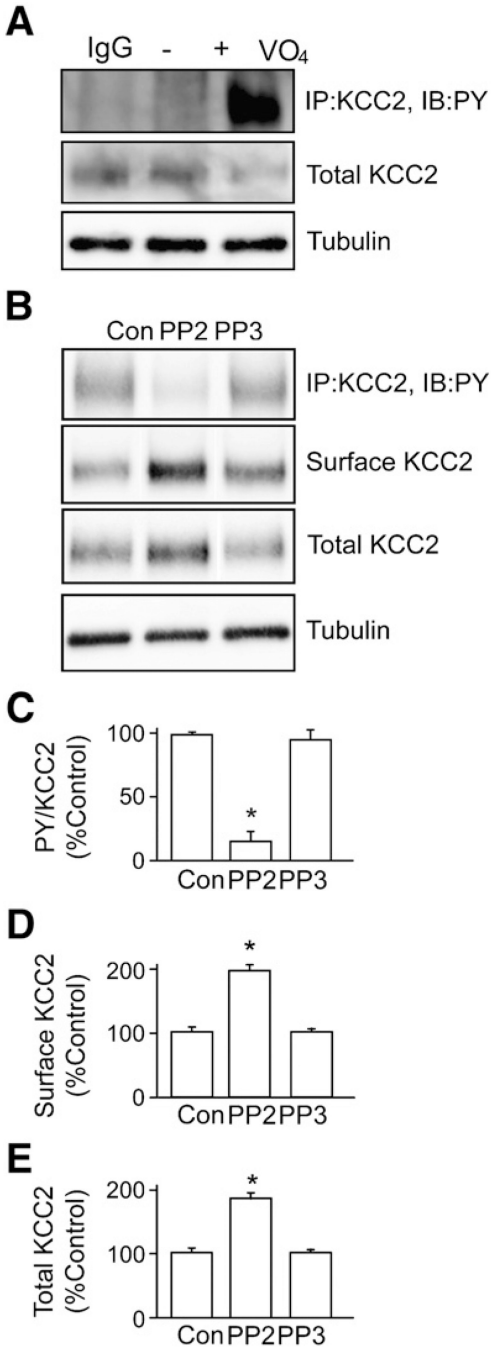

Fig. 3.

Tyrosine phosphorylation of KCC2 is mediated through Src-family tyrosine kinases. A. KCC2 was immunoprecipitated from lysates prepared from hippocampal cultures pretreated with sodium pervanadate (VO_4, 100 μM, 30 min). Tyrosine phosphorylation of immunoprecipitated KCC2 was detected using the PY antibody 4G10. Non-specific rabbit immunoglobulin IgG was used as a negative control for immunoprecipitation. The total amount of KCC2 was also detected using KCC2 antibody. B. An inhibitor of Src-family tyrosine kinases, PP2, or its non-active analog, PP3, was used to pre-treat neurons (20 μM, 30 min) before sodium pervanadate treatment (as above) and immunoprecipitation of KCC2 from cultured neurons followed by immunodetection using PY and KCC2 antibodies. C.

The level of tyrosine phosphorylation of KCC2 was measured by calculating the ratio of the signal of PY to that of KCC2 (PY/KCC2). D. The cell surface levels of KCC2 proteins were measured using biotinylation followed by immunoblotting. E. The total amount of KCC2 was also quantified. In each experiment data were normalized to control. [*Significantly different from control condition ($p<0.01$; value = mean ± SEM, Student's t-test, n = 3)].

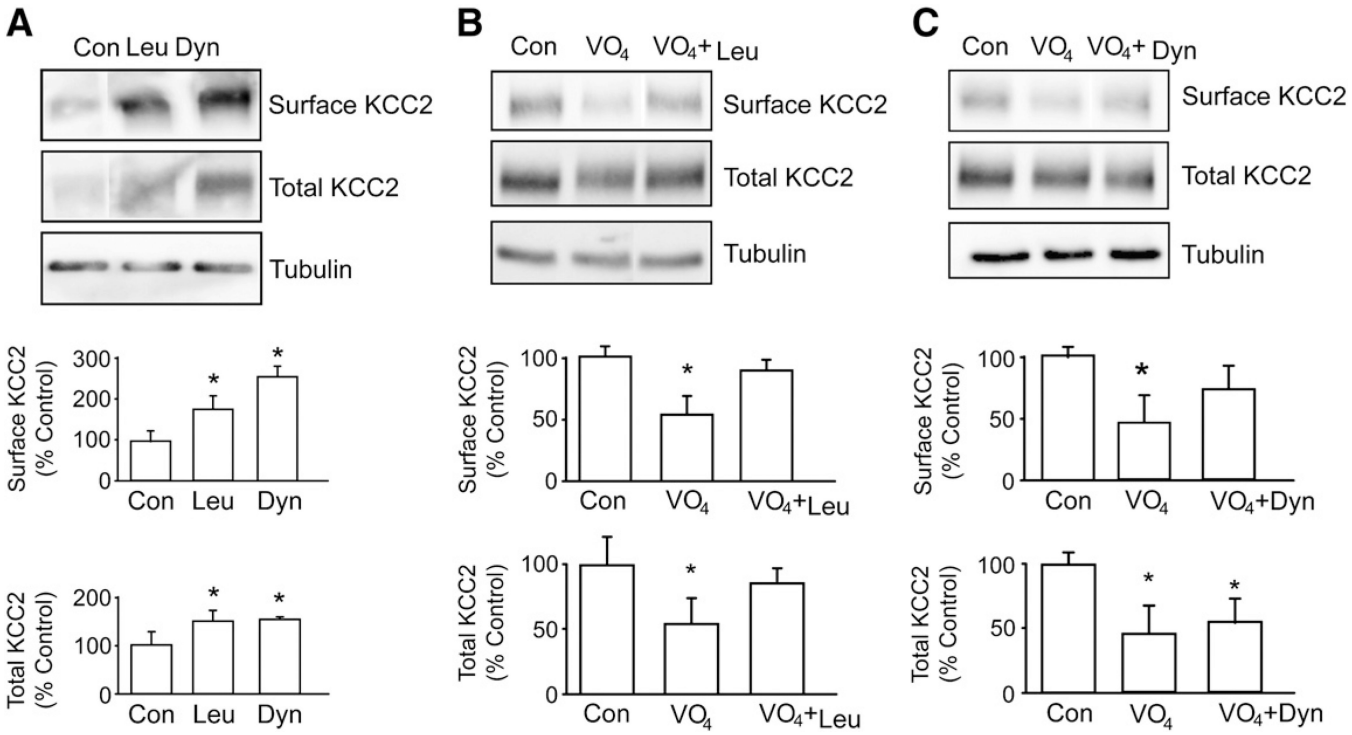

Fig. 4.

Prolonged sodium pervanadate treatment induces removal of KCC2 from the cell surface and results in KCC2 degradation. A. Cultured hippocampal neurons were treated with 200 μg/ml leupeptin or 80 μM dynasore for 45 min. The amount of surface KCC2 protein and that of total KCC2 were analyzed as mentioned above. [*Significantly different from control condition ($p<0.01$; value = mean ± SEM, Student's t-test, n=3)]. B. Cultured hippocampal neurons were treated with sodium pervanadate alone (VO_4, 100 μM, 30 min) or with leupeptin (Leu, 200 μg/ml, 15 min) before treatment with sodium pervanadate. The amount of surface KCC2 protein and that of total KCC2 were analyzed using biotinylation followed by immunoblotting. An equal amount of protein loading was detected by tubulin antibody. C. Cultured hippocampal neurons were treated with sodium pervanadate (VO_4, 100 μM, 30 min) or pre-treated with dynasore (Dyn, 80 μM, 15 min) before treatment with sodium pervanadate. The amount of surface KCC2 protein and that of total KCC2 were analyzed as mentioned above.

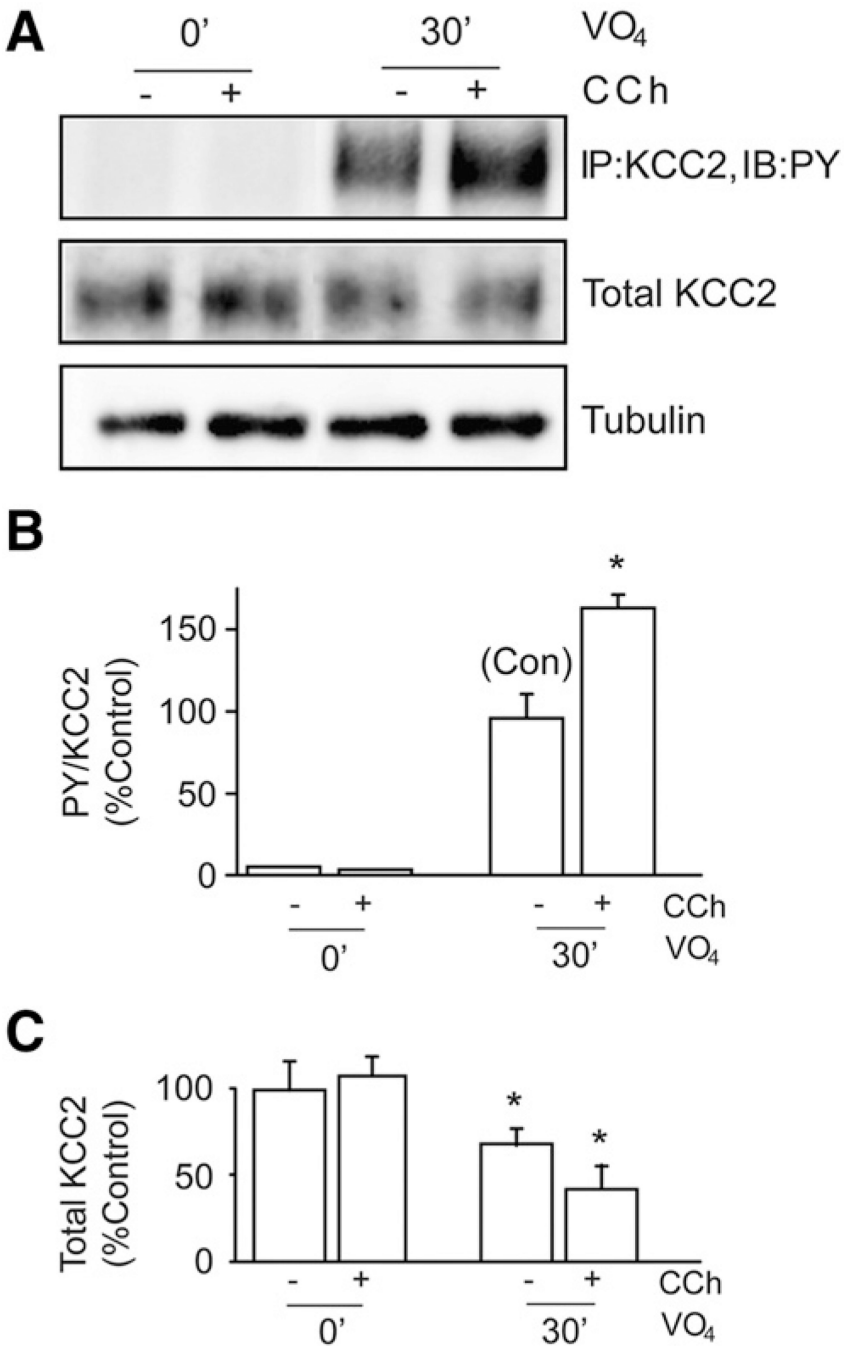

Fig. 5.

Muscarinic activation enhances tyrosine phosphorylation of KCC2 in cultured hippocampal neurons. A. Neurons were treated with carbachol (CCh, 100 μM) together with sodium pervanadate (VO_4, 100 μM) for 30 min. Tyrosine phosphorylation of KCC2 was analyzed by immunoprecipitation of KCC2 followed by immunoblotting with PY antibody. Material was also immunoblotted with tubulin antibodies. The ratio of PY/KCC2 (B) and total KCC2 levels (C) were then measured and normalized to control. [*Significantly different from control condition ($p<0.01$; value = mean ± SEM, Student's t-test, n=3)].

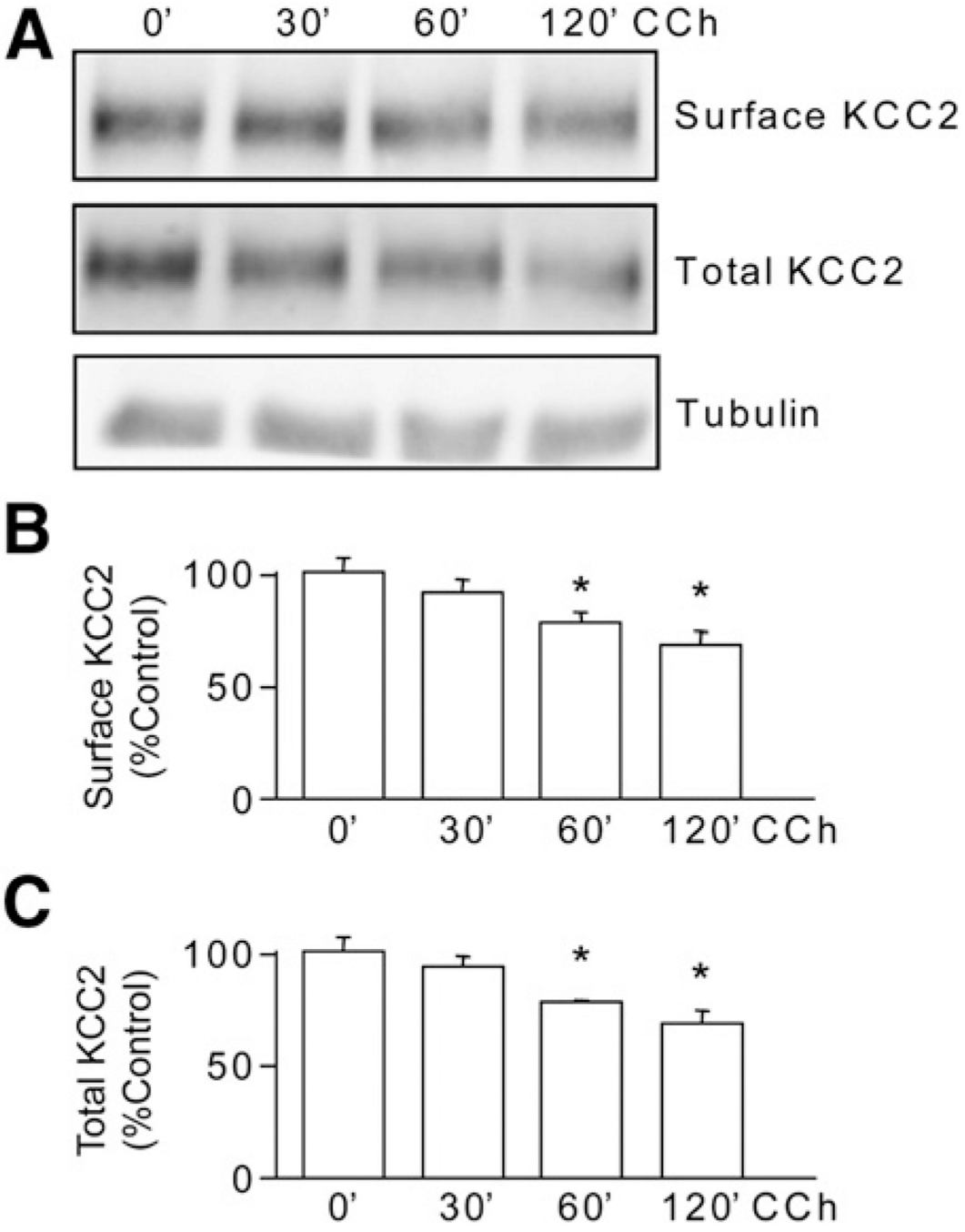

Fig. 6.

Prolonged muscarinic activation induces degradation of KCC2. A. Cultured hippocampal neurons were treated with carbachol (CCh, 100 μM) for up to 120 min. The cell surface and total levels of KCC2 were measured using immunoblotting. Total extracts were also immunoblotted with tubulin antibodies. The levels of cell surface (B) and total levels of KCC2 (C) were then determined and normalized to zero time. [*Significantly different from control condition ($p<0.01$; value = mean ± SEM, Student's t-test, n=3)].

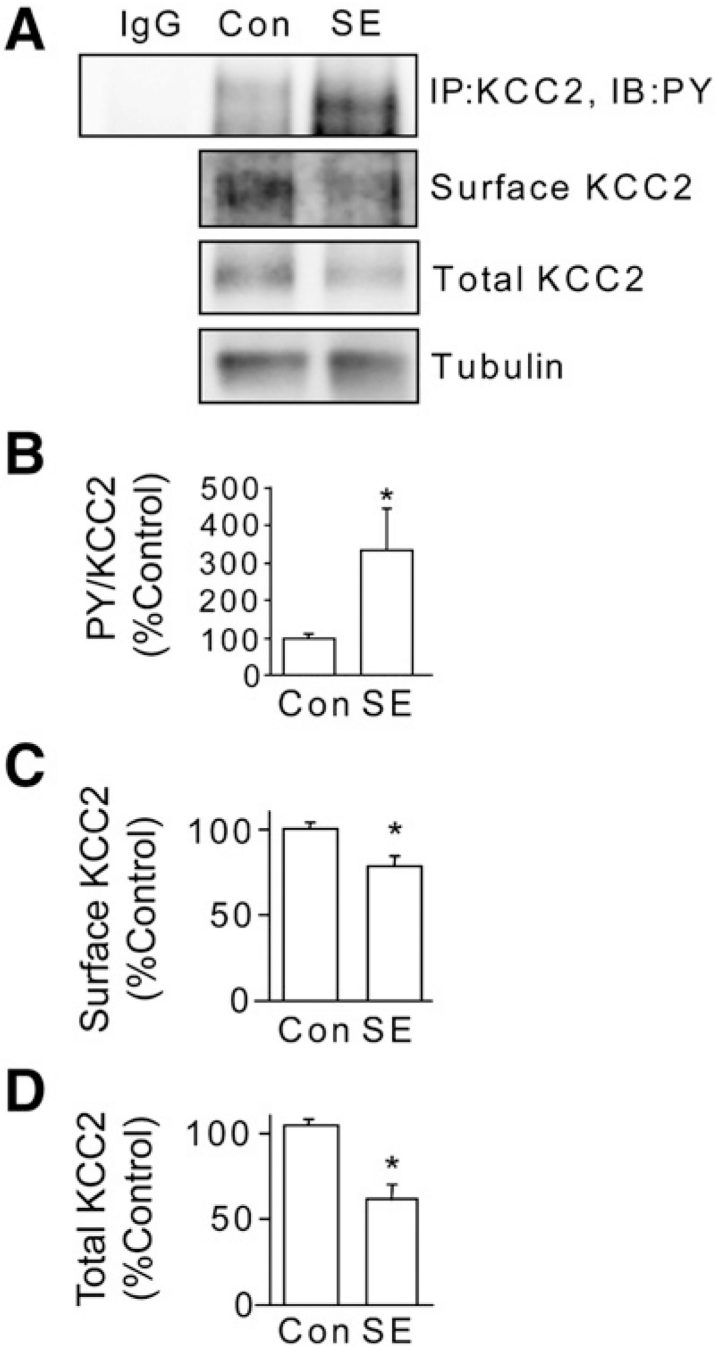

Fig. 7.

Induction of status epilepticus (SE) leads to tyrosine phosphorylation and degradation of KCC2. A. Adult FVB/N mice (8–12 weeks old) were injected with pilocarpine (330 mg/kg) to induce SE. Animals injected with saline were used as controls. Animals that developed SE for 1 h were sacrificed and whole brain 350 mM hippocampal slices were prepared. After incubation some slices were lyzed and KCC2 was immunoprecipitated and immunoblotted with KCC2 antibodies (upper panel). Slices were also labeled with biotin cell surface and total fractions were then immunoblotted with KCC2 antibodies or total fractions were immunoblotted with tubulin antibodies. Non-specific IgG was used as control for immunoprecipitation. These data were then used to calculate the ratio of PY/total KCC2

immunoreactivity (B), cell surface (C) and total levels (D) of KCC2. In each case data were normalized to control. [*Significantly different from control condition ($p<0.01$; value = mean ± SEM, Student's t-test, n=3 mice per group)].